AUT Journal of Modeling and Simulation

AUT J. Model. Simul., 55(2) (2023) 299-316
DOI: 10.22060/miscj.2024.22649.5337

An SDRE- Suboptimal Framework for Robust Control of Multiple Arms Carrying a Load in Cooperation

Neda Nasiri [1], Ahmad Fakharian [1]*, Mohammad Bagher Menhaj [2]

[1] Department of Electrical Engineering, Qazvin Branch, Islamic Azad University, Qazvin, Iran
[2] The Center of Excellence on Control and Robotics, Amirkabir University of Technology (Tehran Polytechnic), Tehran, Iran

ABSTRACT: In this paper, a new application of State-Dependent Riccati Equation (SDRE) is proposed as a framework to design a robust controller for the system of multiple cooperative arms with parametric uncertainties. The cooperative arms are tracking a trajectory holding a mass. Transforming the complicated robust control design to a parallel auxiliary sub-optimal design leads to a considerable facility in design and extensive applicability specifically for complex systems. An auxiliary system with a modified performance criterion is first introduced. The modification in performance criterion is through the incorporation of uncertainties in upper bounds obtained from stability proof. Uncertain State- Dependent Coefficient (USDC) regarding joints' friction for the robotic system is utilized to obtain the auxiliary USDC structure. Two control policies are considered: independent control of each arm and simultaneous control of overall multiple manipulators. The sub-optimal problem for the auxiliary system is solved. The achieved optimal control input for the auxiliary system is the robust input for the equivalent uncertain system. Simulation results in both policies verify the effectiveness and satisfactory robustness (30%) of the proposed scheme in load carrying. Moreover, considering the same trajectory, payload, and design parameters controlling the overall robotic system is superior with respect to separately controlling each arm. Finally, a comparison study is presented for the proposed scheme and Mixed SDRE-SMC (MiSS) for the overall robotic system carrying the same payload through simulation results.

Review History:

Received: Sep. 01, 2023
Revised: Jan. 12, 2024
Accepted: May, 26, 2024
Available Online: May, 30, 2024

Keywords:

Robust Control
Cooperative Manipulators
State-Dependent Riccati Equation
Load Carrying
Dynamic Load Carrying Capacity (DLCC)
Mixed SDRE-SMC (MiSS)

1- Introduction

Hamilton-Jacobi-Bellman (HJB) equation arises in optimal control design, due to applying the principle of optimality to the nonlinear dynamic programming [1-2]. As mentioned in [3], due to the extreme complexity of analytically solving HJB, especially for complicated systems, some techniques have been proposed to approximately solve the problem such as power series expansion [4-5], Adomian decomposition [6], reinforcement learning [7-8], differential transformation [9], State-Dependent Riccati Equation (SDRE) [10] and so on. Regarding the advantages of the SDRE, it has been employed as an approach to optimal control and estimator design for several systems such as robotic systems [11-13], Ebola [14], batteries [15], etc. However, there are a few investigations on robust controller design based on the SDRE [13], [15-19]. Kuo [20] proposed SDRE to solve the robust control problem for chaos synchronization. Nasiri et al. in [21], extended [20] to design an observer-based robust controller for physical systems such as flexible-joint and electrical flexible-joint robotic manipulators in the presence of disturbances. A differential form of SDRE was employed to solve the robust tracking problem for non-affine systems and applied to flexible joint robots [22]. As another robust control scheme based on SDRE, in [18] and [19], SDRE is employed to design the sliding surface and the combined SDRE-SMC applied to cooperative manipulators.

Due to the broad applications of robot manipulators, many controllers have been proposed for robot manipulators in the literature [16-17], [21-27]. However, in some applications such as carrying a load, cooperation between two or more arms has a great deal of importance. To simply illustrate the importance of cooperation in holding an object, as mentioned in [28], imagine a situation in which a few persons intend to carry a load with the same power as one strong person. Obviously, it is superior for the object to be carried with more than one person, in cooperation. Hence, it can be concluded cooperative robotic system is superior in some applications. A system of two manipulators exerts forces on an object to move, referred as multiple arms or robot manipulators in cooperation [29-32].

Inspiring by [16], [20], the main contributions of this paper are:

- Proposing *the application* of SDRE framework to solve the robust control problem for non-affine systems with unmatched and input uncertainties.

*Corresponding author's email: ahmad.fakharian@qiau.ac.ir

• Applying the proposed method to *cooperative manipulators with friction and input saturation holding an object* in two situations: *separately* controlled arms and control of the *overall* system of cooperative manipulators. The control objective is to increase the Dynamic Load Carrying Capacity (DLCC) and track a trajectory with small errors and control effort.

To design the robust controller, an equivalent auxiliary system with a modified cost function is first considered. Then by using the SDRE, the parallel suboptimal problem is solved. The solution to the parallel problem is the robust control input. This technique considerably facilitates the procedure of solving the complicated robust control problem. The main novelty of this work is to apply the simplifying procedure given in [16], [20] for robust control of multiple cooperative arms handling an object to increase DLCC. The results are compared in both situations to indicate the superiority of simultaneous robust control of the robotic system with respect to independent robust control of each arm. Furthermore, to verify the superiority of the proposed robust controller versus SDRE-based SMC simulation results are compared. A comparison among SDRE-based optimal and robust schemes for cooperative manipulators with this study is presented in Table 1.

This paper is organized as follows; in section 2 the structure of the robust SDRE-based controller and stability proof are given. In section 3, the dynamics of cooperative manipulators are presented. Section 4, is dedicated to robust SDRE-based controller design for cooperative manipulators using two policies: independent robust SDRE-based control and simultaneous robust SDRE-based control for the overall system. In section 5, simulations for both cases are presented, compared with each other and SDRE-based SMC. Finally, section 6, concludes the paper.

2- Proposed Robust Controller Design

Consider the non-linear non-affine system as:

$$\dot{\mathbf{x}}(t) = \mathbf{f}(\mathbf{x}(t), \boldsymbol{\upsilon}) + \mathbf{g}(\mathbf{x}(t), \mathbf{u}(t), \boldsymbol{\upsilon})$$
$$\boldsymbol{y}(t) = \mathbf{h}(\mathbf{x}(t)) \tag{1}$$

where $\mathbf{x}(t) \in \mathcal{R}^n$ is the vector of states; $\mathbf{u}(t) \in \mathcal{R}^m$ is the vector of inputs; $\mathbf{y}(t) \in \mathcal{R}^p$ denotes the vector of outputs; $\nu \in \mathcal{R}^n$ indicates the vector of parametric uncertainties.

Assumption 1: $\mathbf{f}(\mathbf{x}(t), \upsilon) \in \mathcal{R}^n$ and $\mathbf{g}(\mathbf{x}(t), \mathbf{u}(t), \upsilon) \in \mathcal{R}^n$ are smooth Lipschitz and piecewise continuous functions.

The first step is to shape the Uncertain State-Dependent Coefficient (USDC) representation for Eq. (1) as:

$$\dot{\mathbf{x}}(t) = \mathbf{A}(\mathbf{x}(t), \boldsymbol{\upsilon})\mathbf{x}(t) + \mathbf{B}(\mathbf{x}(t), \mathbf{u}(t), \boldsymbol{\upsilon})\mathbf{u}(t)$$
$$\boldsymbol{y}(t) = \mathbf{C}(\mathbf{x}(t))\mathbf{x}(t) \tag{2}$$

where $\mathbf{A}(x(t), \upsilon) \in \mathcal{R}^{n\times n}$, $B(x(t), u(t), \upsilon) \in \mathcal{R}^{n\times m}$ and $\mathbf{C}(\mathbf{x}(t)) \in \mathcal{R}^{p\times n}$ are USDC matrix functions. Furthermore, $B(x(t), u(t), \upsilon) = B(x(t), u(t))\Omega(\upsilon)$ where $\Omega(\upsilon) \in \mathcal{R}^{m\times m}$ is the matrix of uncertainty in the input matrix and $\mathbf{B}(\mathbf{x}(t), \mathbf{u}(t)) \in \mathcal{R}^{n\times m}$.

Assumption 2: The pair of $\{A(x(t), \upsilon), B(x(t), u(t), \upsilon)\}$ is pointwise stabilizable and the pair of $\{A(x(t), \upsilon), C(x(t))\}$ is pointwise detectable [16], [20].

Assumption 3: The uncertain system matrix $A(x(t), \upsilon)$ is bounded [16], [20].

Considering [16], and [20] for affine systems, the second step is to define a subsidiary system as follows for non-affine systems:

$$\dot{\mathbf{x}}(t) = \mathbf{A}(\mathbf{x}(t), \boldsymbol{\upsilon}_0)\mathbf{x}(t)$$
$$+\widetilde{\mathbf{B}}(\mathbf{x}(t), \mathbf{u}_{total}(t), \boldsymbol{\upsilon}_0)\mathbf{u}_{total}(t) \tag{3}$$

where $\mathbf{u}_{total}(t)$ is combined control input consists of control input $\mathbf{u}(t) \in \mathcal{R}^m$ and an augmented input $\bar{\mathbf{u}}(t) \in \mathcal{R}^n$ to cope with the uncertainties. Moreover, $\tilde{B}(x(t), u_{total}(t), \upsilon_0)$ is defined as:

$$\widetilde{\mathbf{B}}(\mathbf{x}(t), \mathbf{u}_{total}(t), \boldsymbol{\upsilon}_0) = [\mathbf{B}(\mathbf{x}(t), \mathbf{u}(t), \boldsymbol{\upsilon}_0) \quad \bar{a}(\mathbf{I} - \mathbf{B}(\mathbf{x}(t), \mathbf{u}(t), \boldsymbol{\upsilon}_0)\mathbf{B}^{\#}(\mathbf{x}(t), \mathbf{u}(t), \boldsymbol{\upsilon}_0))] \tag{4}$$

and the subsidiary USDC of the system (1) is obtained using Eqs. (3) and (4):

$$\dot{\mathbf{x}}(t) = \mathbf{A}(\mathbf{x}(t), \boldsymbol{\upsilon}_0)\mathbf{x}(t) + \mathbf{B}(\mathbf{x}(t), \mathbf{u}(t), \boldsymbol{\upsilon}_0)\mathbf{u}(t)$$
$$+\bar{a}\left(\mathbf{I} - \mathbf{B}(\mathbf{x}(t), \mathbf{u}(t), \boldsymbol{\upsilon}_0)\mathbf{B}^{\#}(\mathbf{x}(t), \mathbf{u}(t), \boldsymbol{\upsilon}_0)\right)\bar{\mathbf{u}}(t) \tag{5}$$

where $B(x(t), u(t), \upsilon_0) = B(x(t), u(t))\Omega$, the nominal value $\upsilon_0 \in \underline{\upsilon}$ and $\Omega \in \Omega(\upsilon)$ is positive constant matrix, furthermore a is a positive constant and $B^{\#}(x(t), u(t), \upsilon_0) = \left(B^{\mathrm{T}}(x(t), u(t), \upsilon_0)B(x(t), u(t), \upsilon_0)\right)^{-1} \times B^{\mathrm{T}}(x(t), u(t), \upsilon_0)$ [20].

The Third step is to reflect the uncertainties upper bounds in the cost function for subsidiary system Eq. (5) as given in [16]:

$$J = \int_0^{\infty} \{\mathbf{x}^{\mathrm{T}}(t)\widehat{\mathbf{Q}}(\mathbf{x}(t))\mathbf{x}(t) + \mathbf{u}_{total}^{\mathbf{T}}(t)\widehat{\mathbf{R}}\mathbf{u}_{total}(t)\}dt \tag{6}$$

Table 1. Comparison the SDRE-based schemes for cooperative manipulators with presented work

Reference	Method	Performance Index, Control input	Novelty Description
[12]	Optimal control based on SDRE	$\mathrm{J}=\int_0^\infty(\mathbf{x}^{\mathrm{T}}(t)\mathbf{Q}\mathbf{x}(t)+\mathbf{u}^{\mathrm{T}}(t)\mathbf{R}\mathbf{u}(t))\,dt$ $\boldsymbol{u}(t)=-\mathbf{R}^{-1}\mathbf{B}^{\mathrm{T}}\mathbf{K}\mathbf{X}$	▪ Increasing DLCC for cooperative manipulators using SDRE
[18]	Robust control based on combining SDRE and SMC	$\mathrm{J}=\frac{1}{2}(\mathbf{x}^{\mathrm{T}}(t_f)\mathbf{F}\mathbf{x}(t_f)+\int_0^{t_f}(\mathbf{x}^{\mathrm{T}}(t)\mathbf{Q}\mathbf{x}(t)+\mathbf{u}^{\mathrm{T}}(t)\mathbf{R}\mathbf{u}(t))\,dt$ $\boldsymbol{u}(\boldsymbol{t})=(\mathbf{B}^{\mathrm{T}}\mathbf{K}\mathbf{B})^{-1}(\mathbf{B}^{\mathrm{T}}\mathbf{K}\dot{\mathbf{x}}_{des}-\dot{\mathbf{B}}^{\mathrm{T}}\mathbf{K}\tilde{\mathbf{x}}-\mathbf{B}^{\mathrm{T}}\dot{\mathbf{K}}\tilde{\mathbf{x}}-\mathbf{B}^{\mathrm{T}}\mathbf{K}\mathbf{f}-\mathbf{K}_{\mathrm{Corr}}\mathbf{sgn}(\mathbf{s}))$ $\boldsymbol{u}(t)=-\mathbf{R}^{-1}\mathbf{B}^{\mathrm{T}}\mathbf{K}\mathbf{x}-\mathbf{K}_{\mathrm{Corr}}\mathbf{sgn}(\mathbf{s})$	▪ Combining SMC and SDRE by considering the SDRE in design of the algebraic sliding surface. ▪ Increasing dynamic load carrying capacity of cooperative manipulators
[19]			▪ Combining SMC and SDRE by considering the SDRE in design of algebraic and integral sliding surfaces ▪ Providing robust attitude with desired finite-time control option for cooperative manipulators
[22]	Robust SDDRE-based control for trajectory tracking	$J=\frac{1}{2}[\mathbf{y}(t_f)-\mathbf{y}_d(t_f)]^{\mathrm{T}}\mathbf{F}[\mathbf{y}(t_f)-\mathbf{y}_d(t_f)]$ $+\frac{1}{2}\int_0^{t_f}\{[\boldsymbol{y}(t)-\boldsymbol{y}_d(t)]^{\mathrm{T}}\overline{\mathbf{Q}}(\mathbf{X}(t),t)[\boldsymbol{y}(t)-\boldsymbol{y}_d(t)]$ $+\mathbf{U}^{\mathrm{T}}(t)\overline{\mathbf{R}}(\mathbf{X}(t),t)\mathbf{U}(t)\}$ $\overline{\mathbf{Q}}(\mathbf{X}(t),t)=\mathbf{M}+a^2\mathbf{H}+b^2\mathbf{S}+c^2\widetilde{\mathbf{Q}}(\mathbf{X}(t),t)$ $\overline{\mathbf{R}}(\mathbf{X}(t),t)=\begin{bmatrix}\widetilde{\mathbf{R}}(\mathbf{X}(t),t) & 0\\ 0 & (a^2+b^2)\mathbf{I}\end{bmatrix}$ and: $\mathbf{U}(t)=\begin{bmatrix}\mathbf{u}(t)\\ \overline{\mathbf{u}}(t)\end{bmatrix}=-\mathbf{R}^{-1}(\mathbf{X}(t),t)\overline{\overline{\mathbf{B}}}^{\mathrm{T}}(\mathbf{X}(t),\mathbf{U}(t),\boldsymbol{\eta}_0,t)\big(\mathbf{K}(\mathbf{X}(t),\mathbf{U}(t),t)\mathbf{X}(t)$ $+\mathbf{Z}(\mathbf{X}(t),\mathbf{U}(t),t)\big)$ where: $\overline{\overline{\mathbf{B}}}(\mathbf{X}(t),\mathbf{U}(t),\boldsymbol{\eta}_0,t)$ $=[\mathbf{B}(\mathbf{X}(t),\mathbf{U}(t),\boldsymbol{\eta}_0,t)\quad(\mathbf{I}-\mathbf{B}(\mathbf{X}(t),\mathbf{U}(t),\boldsymbol{\eta}_0,t)\mathbf{B}^{+}(\mathbf{X}(t),\mathbf{U}(t),\boldsymbol{\eta}_0,t))(\bar{\mathrm{a}}+\bar{\mathrm{b}}\mathbf{W})]$	▪ Proposing differential SDRE to solve the robust tracking control for non-affine time-dependent systems with input and mismatched uncertainty. ▪ Applying the proposed scheme to flexible-joint manipulators for trajectory tracking
This work	Robust SDRE-based control for increasing DLCC	$\mathrm{J}=\int_0^\infty\{\mathbf{x}^{\mathrm{T}}(t)\widehat{\mathbf{Q}}(\mathbf{x}(t))\mathbf{x}(t)+\mathbf{u}_{total}^{\mathbf{T}}(t)\widehat{\mathbf{R}}(\mathbf{x}(t))\mathbf{u}_{total}(t)\}dt$ where: $\widehat{\mathbf{Q}}(\mathbf{X}(t))=\mathbf{H}+a^2\mathbf{M}+c^2\mathbf{Q}(\mathbf{X}(t))$ $\widehat{\mathbf{R}}(\mathbf{X}(t))=\begin{bmatrix}\mathbf{R}(\mathbf{x}(t)) & 0\\ 0 & (a^2+b^2)\mathbf{I}\end{bmatrix}$ and**:** $\mathbf{u}_{total}(t)=\begin{bmatrix}\mathbf{u}(t)\\ \overline{\mathbf{u}}(t)\end{bmatrix}=-\widehat{\mathbf{R}}^{-1}(\mathbf{x}(t))\widetilde{\mathbf{B}}^{\mathrm{T}}(\mathbf{x}(t),\boldsymbol{\upsilon}_0)\mathbf{K}(\mathbf{x}(t))\mathbf{x}(t)$ $=\begin{bmatrix}-\mathbf{R}^{-1}\mathbf{B}^{\mathrm{T}}(\mathbf{x}(t),\mathbf{u}(t),\boldsymbol{\upsilon}_0)\\ -(a^2+b^2)^{-1}\bar{a}[\mathbf{I}-\mathbf{B}(\mathbf{x}(t),\mathbf{u}(t),\boldsymbol{\upsilon}_0)\mathbf{B}^{\#}(\mathbf{x}(t),\mathbf{u}(t),\boldsymbol{\upsilon}_0)]^{\mathrm{T}}\end{bmatrix}\mathbf{K}(\mathbf{x}(t),\mathbf{u}_{total}(t),\mathbf{x}(t))$ where: $\widetilde{\mathbf{B}}(\mathbf{x}(t),\mathbf{u}_{total}(t),\boldsymbol{\upsilon}_0)$ $=[\mathbf{B}(\mathbf{x}(t),\mathbf{u}(t),\boldsymbol{\upsilon}_0)\quad\bar{a}(\mathbf{I}-\mathbf{B}(\mathbf{x}(t),\mathbf{u}(t),\boldsymbol{\upsilon}_0)\mathbf{B}^{\#}(\mathbf{x}(t),\mathbf{u}(t),\boldsymbol{\upsilon}_0))]$	▪ Proposing a robust controller in an SDRE-based optimal framework for cooperative manipulators to increase DLCC. ▪ Considering two situations to design the controller: independent robust control for each arm and simultaneous control of overall dual-arms system regarding friction and input saturation. ▪ Comparing the results with MiSS to illustrate superiority of the proposed scheme

where weighting matrices $\hat{\mathbf{Q}}(\mathbf{x}(t))$ (which is symmetric positive semi-definite) and $\hat{\mathbf{R}}$ (which is symmetric positive definite) are formed using subsidiary weighting matrices for states $\mathbf{Q}>0$ and for inputs $\mathbf{R}>0$ in the cost function Eq. (6) and the uncertainties upper bounds are reflected in the performance criterion through modifying design weighting matrices as:

$$\hat{\mathbf{Q}}(\mathbf{x}(t)) = \mathbf{H} + a^2\mathbf{M} + c^2\mathbf{Q} \tag{7}$$

$$\hat{\mathbf{R}} = \begin{bmatrix} \mathbf{R} & 0 \\ 0 & (a^2+b^2)\mathbf{I} \end{bmatrix} \tag{8}$$

in which $a, b, c \geq 0$ are constant parameters and the upper bounds for mismatched uncertainties are obtained using subsequent stability analysis as :

$$(\mathbf{B}^{\#}(\mathbf{x}(t),\mathbf{u}(t),\boldsymbol{\upsilon}_0)\mathbf{A}(\mathbf{x}(t),\boldsymbol{\upsilon},\boldsymbol{\upsilon}_0))^{\mathrm{T}}\mathbf{R}\mathbf{B}^{\#}(\mathbf{x}(t),\mathbf{u}(t),\boldsymbol{\upsilon}_0)\mathbf{A}(\mathbf{x}(t),\boldsymbol{\upsilon},\boldsymbol{\upsilon}_0) \leq \mathbf{H}\,, \tag{9}$$

$$\bar{a}^{-2}\mathbf{A}^{\mathrm{T}}(\mathbf{x}(t),\boldsymbol{\upsilon},\boldsymbol{\upsilon}_0)\mathbf{A}(\mathbf{x}(t),\boldsymbol{\upsilon},\boldsymbol{\upsilon}_0) \leq \mathbf{M}. \tag{10}$$

Auxiliary weighting matrices $\mathbf{R}$ and $\mathbf{Q}$ have been considered to increase design flexibility for inputs and states, respectively.

The augmented control input $\mathbf{u}_{total}(t)$ is as given in [16]:

$$\begin{aligned}\mathbf{u}_{total}(t) &= \begin{bmatrix}\mathbf{u}(t)\\ \bar{\mathbf{u}}(t)\end{bmatrix} = -\hat{\mathbf{R}}^{-1}\tilde{\mathbf{B}}^{\mathrm{T}}(\mathbf{x}(t),\mathbf{u}_{total}(t),\boldsymbol{\upsilon}_0)\mathbf{K}(\mathbf{x}(t),\mathbf{u}_{total}(t))\mathbf{x}(t)\\ &= \begin{bmatrix}-\mathbf{R}^{-1}\mathbf{B}^{\mathrm{T}}(\mathbf{x}(t),\mathbf{u}(t),\boldsymbol{\upsilon}_0)\\ -(a^2+b^2)^{-1}\bar{a}[\mathbf{I}-\mathbf{B}(\mathbf{x}(t),\mathbf{u}(t),\boldsymbol{\upsilon}_0)\mathbf{B}^{\#}(\mathbf{x}(t),\mathbf{u}(t),\boldsymbol{\upsilon}_0)]^{\mathrm{T}}\end{bmatrix}\\ &\times \mathbf{K}(\mathbf{x}(t),\mathbf{u}_{total}(t))\mathbf{x}(t)\end{aligned} \tag{11}$$

in which $\mathbf{K}(\mathbf{x}(t))$ is the solution of the Uncertain SDRE (USDRE):

$$\begin{aligned}\dot{\mathbf{K}}(\mathbf{x}(t),\mathbf{u}_{total}(t)) &= -\mathbf{K}(\mathbf{x}(t),\mathbf{u}_{total}(t))\mathbf{A}(\mathbf{x}(t),\boldsymbol{\upsilon}_0)\\ &-\mathbf{A}^{\mathrm{T}}(\mathbf{x}(t),\boldsymbol{\upsilon}_0)\mathbf{K}(\mathbf{x}(t),\mathbf{u}_{total}(t))\\ &+\mathbf{K}(\mathbf{x}(t),\mathbf{u}_{total}(t))\tilde{\mathbf{B}}(\mathbf{x}(t),\mathbf{u}(t),\boldsymbol{\upsilon}_0)\\ &\hat{\mathbf{R}}^{-1}\tilde{\mathbf{B}}^{\mathrm{T}}(\mathbf{x}(t),\mathbf{u}(t),\boldsymbol{\upsilon}_0)\mathbf{K}(\mathbf{x}(t),\mathbf{u}_{total}(t))\\ &-\mathbf{C}^{\mathrm{T}}(\mathbf{x}(t))\hat{\mathbf{Q}}(\mathbf{x}(t))\mathbf{C}(\mathbf{x}(t))\end{aligned} \tag{12}$$

Now, the objective is to prove SDRE as an optimal framework can be used to obtain robust control input by modifying the performance index and input matrix. Moreover, the upper bounds of uncertainty Eqs. (9) and (10) are obtained using stability proof.

Note: In order to simplify the notations, in this paper, $(\mathbf{x}(t),\mathbf{u}(t))$ is replaced with $(.)$.

2- 1- Stability Proof

Theorem: Consider the *robust control problem* for the *nonlinear non- affine* system (1) to be solved. Towards this aim, regarding assumptions (1)-(3), the *equivalent sub optimal problem* for the *subsidiary USDC structure* (5) must be solved. If:

1- The design parameters $\bar{a}$, a , b , c and the subsidiary weighting matrices $\mathbf{Q}$ and $\mathbf{R}$ can be chosen in such a way the solution to the sub-optimal control problem, $\mathbf{u}_{total}(t)$ in Eq.(11) exists;

2- The necessary condition $c^2Q-2(a^2+b^2)\Omega^{\mathrm{T}}\Omega>0$ be satisfied where $\grave{\mathbf{U}}$ is the feedback gain of $\bar{\mathbf{u}}(t)$ element of $\mathbf{u}_{total}(t)$;

then the $\mathbf{u}(t)$ part of $\mathbf{u}_{total}(t)$ is the solution of the robust control problem.

Proof:

The objective is to prove SDRE as an optimal framework can be used to obtain robust control input by modifying the performance index and input matrix. Mimicking the selected Lyapunov function for LQR-based robust control in [33], the Lyapunov function is defined as the minimum performance index with incorporation of uncertainties upper bounds with modification:

$$\mathbf{V}(\mathbf{x}) = min_{\bar{\mathbf{u}},\bar{\mathbf{u}}}\int_0^{\infty}(\mathbf{x}^{\mathrm{T}}(\mathbf{H}+a^2\mathbf{M}+c^2\mathbf{Q})\mathbf{x}+\mathbf{u}^{\mathrm{T}}\mathbf{R}\mathbf{u} + \bar{\mathbf{u}}^{\mathrm{T}}(a^2+b^2)\bar{\mathbf{u}})dt \tag{13}$$

$\mathbf{V}(\mathbf{x})$ should be satisfied in the Hamilton-Jacobi-Bellman equation [32]. Therefore, considering the equivalent subsidiary USDC structure Eq. (3), Eq. (14) is obtained:

$$\begin{aligned} & min_{\mathbf{u}_{total}}(\mathbf{x}^{\mathrm{T}}(\mathbf{H}+a^2\mathbf{M}+c^2\mathbf{Q})\mathbf{x} \\ & +\mathbf{u}^{\mathbf{T}}\mathbf{R}\mathbf{u}+\overline{\mathbf{u}}^{\mathbf{T}}(a^2 \ +b^2)\overline{\mathbf{u}}) \\ & +\mathbf{V}_{\mathrm{x}}^{\mathrm{T}}(\mathbf{A}(\mathbf{x}(t),\boldsymbol{\upsilon}_0)\mathbf{X}(t)+\mathbf{B}(.,\boldsymbol{\upsilon}_0)\mathbf{u}(t) \\ & +\bar{a}\left(\mathbf{I}-\mathbf{B}(.,\boldsymbol{\upsilon}_0)\mathbf{B}^{\#}(.,\boldsymbol{\upsilon}_0)\right)\overline{\mathbf{u}}(t))=0 \end{aligned} \tag{14}$$

Hence, the derivative with respect to $\mathbf{u}$ and $\overline{\mathbf{u}}$ must be equal to zero. As a result:

$$2\mathbf{u}^{\mathbf{T}}\mathbf{R}+\mathbf{V}_{\mathrm{x}}^{\mathrm{T}}\mathbf{B}(.,\boldsymbol{\upsilon}_0)=0 \tag{15}$$

$$2(a^2 \ +b^2)\overline{\mathbf{u}}^{\mathrm{T}}+\mathbf{V}_{\mathrm{x}}^{\mathrm{T}}\bar{a}\left(\mathbf{I}-\mathbf{B}(.,\boldsymbol{\upsilon}_0)\mathbf{B}^{\#}(.,\boldsymbol{\upsilon}_0)\right)=0 \tag{16}$$

Considering the time derivative of $\mathbf{V}(\mathbf{x})$, substituting Eq. (2) and adding and subtracting $B(.,\upsilon_0)u$, regarding $B(.,\upsilon)=B(.)\Omega(\upsilon)$ and $B(.,\upsilon_0)=B(.)\Omega$ we have:

$$\begin{aligned} & \dot{\mathbf{V}}(\mathbf{x})=\mathbf{V}_{\mathrm{x}}^{\mathrm{T}}\dot{\mathbf{X}}=\mathbf{V}_{\mathrm{x}}^{\mathrm{T}}(\mathbf{A}(\mathbf{x}(t),\boldsymbol{\upsilon})\mathbf{x}(t)+\mathbf{B}(.,\boldsymbol{\upsilon})\mathbf{u}) \\ & =\mathbf{V}_{\mathrm{X}}^{\mathrm{T}}(\mathbf{A}(\mathbf{x}(t),\boldsymbol{\upsilon}_0)\mathbf{x}(t)+\mathbf{A}(\mathbf{x}(t),\boldsymbol{\upsilon},\boldsymbol{\upsilon}_0) \\ & +(\mathbf{I}+\frac{\boldsymbol{\Omega}(\boldsymbol{\upsilon})-\Omega}{\boldsymbol{\Omega}})\mathbf{B}(.,\boldsymbol{\upsilon}_0)\mathbf{u}) \end{aligned} \tag{17}$$

where $\mathbf{V}_{\mathrm{x}}=\frac{\partial\mathbf{V}(\mathbf{x})}{\partial\mathbf{x}}$. Substituting Eq. (15), $\dot{\mathbf{V}}(\mathbf{x})$ can be rewritten as:

$$\begin{aligned} & \dot{\mathbf{V}}(\mathbf{x})=\mathbf{V}_{\mathrm{x}}^{\mathrm{T}}(\mathbf{A}(\mathbf{x}(t),\boldsymbol{\upsilon}_0)\mathbf{x}(t) \\ & +\mathbf{A}(\mathbf{x}(t),\boldsymbol{\upsilon},\boldsymbol{\upsilon}_0)+\mathbf{B}(.,\boldsymbol{\upsilon}_0)\mathbf{u})-2(\frac{\boldsymbol{\Omega}(\boldsymbol{\Xi})-\boldsymbol{\Omega}}{\boldsymbol{\Omega}})\mathbf{u}^{\mathbf{T}}\mathbf{R}\mathbf{u} \\ & \leq\mathbf{V}_{\mathrm{X}}^{\mathrm{T}}\big(\mathbf{A}(\mathbf{x}(t),\boldsymbol{\upsilon}_0)\mathbf{X}+\mathbf{B}(.,\boldsymbol{\upsilon}_0)\mathbf{u}+\mathbf{A}(\mathbf{x}(t),\boldsymbol{\upsilon},\boldsymbol{\upsilon}_0)\big) \end{aligned} \tag{18}$$

Adding and subtracting $V_{\mathrm{x}}^{\mathrm{T}}B(.,\upsilon_0)B^{\#}(.,\upsilon_0)A(x(t),\upsilon,\upsilon_0)$ and $V_{\mathrm{x}}^{\mathrm{T}}\left(I-B(.,\upsilon_0)B^{\#}(.,\upsilon_0)\right)\overline{au}$ to Eq. (18), with slight manipulation, Eq. (19) is obtained.

$$\begin{aligned} & \dot{\mathbf{V}}(\mathbf{x})\leq\mathbf{V}_{\mathrm{x}}^{\mathrm{T}}(\mathbf{A}(\mathbf{x}(t),\boldsymbol{\upsilon}_0)\mathbf{x}(t) \\ & \quad +\mathbf{B}(.,\boldsymbol{\upsilon}_0)\mathbf{u}+\left(\mathbf{I}-\mathbf{B}(.,\boldsymbol{\upsilon}_0)\mathbf{B}^{\#}(.,\boldsymbol{\upsilon}_0)\right)\overline{\mathbf{u}}) \\ & \quad +\mathbf{V}_{\mathrm{x}}^{\mathrm{T}}\mathbf{A}(\mathbf{x}(t),\boldsymbol{\upsilon},\boldsymbol{\upsilon}_0)-\mathbf{V}_{\mathrm{x}}^{\mathrm{T}}\left(\mathbf{I}-\mathbf{B}(.,\boldsymbol{\upsilon}_0)\mathbf{B}^{\#}(.,\boldsymbol{\upsilon}_0)\right)\overline{\mathbf{u}} \\ & \quad +\mathbf{V}_{\mathrm{x}}^{\mathrm{T}}\mathbf{B}(.,\boldsymbol{\upsilon}_0)\mathbf{B}^{\#}(.,\boldsymbol{\upsilon}_0)\big(\mathbf{A}(\mathbf{x}(t),\boldsymbol{\upsilon},\boldsymbol{\upsilon}_0)\big) \\ & \quad -\mathbf{V}_{\mathrm{x}}^{\mathrm{T}}\mathbf{B}(.,\boldsymbol{\upsilon}_0)\mathbf{B}^{\#}(.,\boldsymbol{\upsilon}_0)\mathbf{A}(\mathbf{x}(t),\boldsymbol{\upsilon},\boldsymbol{\upsilon}_0) \end{aligned} \tag{19}$$

Replacing Eqs. (15) and (16) into Eq. (19) and some slight changes in arrangement, Eq. (20) yields:

$$\begin{aligned} & \dot{\mathbf{V}}(\mathbf{x})\leq\mathbf{V}_{\mathrm{x}}^{\mathrm{T}}(\mathbf{A}(\mathbf{x}(t),\boldsymbol{\upsilon}_0)\mathbf{x}(t)+\mathbf{B}(.,\boldsymbol{\upsilon}_0)\mathbf{u} \\ & \quad +\left(\mathbf{I}-\mathbf{B}(.,\boldsymbol{\upsilon}_0)\mathbf{B}^{\#}(.,\boldsymbol{\upsilon}_0)\right)\bar{a}\overline{\mathbf{u}}) \\ & \quad +2(a^2+b^2)\overline{\mathbf{u}}^{\mathrm{T}}\overline{\mathbf{u}} \\ & \quad -2\mathbf{u}^{\mathbf{T}}\mathbf{R}\,\mathbf{B}^{\#}(.,\boldsymbol{\upsilon}_0)\mathbf{A}(\mathbf{x}(t),\boldsymbol{\upsilon},\boldsymbol{\upsilon}_0)+\mathbf{V}_{\mathrm{x}}^{\mathrm{T}} \\ & \quad \times\left(\mathbf{I}-\mathbf{B}(.,\boldsymbol{\upsilon}_0)\mathbf{B}^{\#}(.,\boldsymbol{\upsilon}_0)\right)\mathbf{A}(\mathbf{x}(t),\boldsymbol{\upsilon},\boldsymbol{\upsilon}_0) \end{aligned} \tag{20}$$

Now Eq. (20) can be rewritten as Eq. (21):

$$\begin{aligned} & \dot{\mathbf{V}}(\mathbf{x})\leq-\mathbf{x}^{\mathrm{T}}(\mathbf{H}+a^2\mathbf{M}+c^2\mathbf{Q})\mathbf{x}-\mathbf{u}^{\mathbf{T}}\mathbf{R}\mathbf{u} \\ & \quad -\overline{\mathbf{u}}^{\mathrm{T}}(a^2+b^2)\overline{\mathbf{u}}+2b^2\overline{\mathbf{u}}^{\mathrm{T}}\overline{\mathbf{u}} \\ & \quad -2\mathbf{u}^{\mathbf{T}}\widetilde{\mathbf{R}}\,\mathbf{B}^{\#}(.,\boldsymbol{\upsilon}_0)\mathbf{A}(\mathbf{x}(t),\boldsymbol{\upsilon},\boldsymbol{\upsilon}_{\mathbf{0}}) \\ & \quad -2\overline{\mathbf{u}}^{\mathrm{T}}\bar{a}^{-1}a^2\mathbf{A}(\mathbf{x}(t),\boldsymbol{\upsilon},\boldsymbol{\upsilon}_{\mathbf{0}}) \end{aligned} \tag{21}$$

Hence, one can represent Eq. (21) as:

$$\begin{aligned} & \dot{\mathbf{V}}(\mathbf{x})\leq-\mathbf{x}^{\mathrm{T}}(\mathbf{H}+a^2\mathbf{M}+c^2\mathbf{Q})\mathbf{x} \\ & \quad -\left(\mathbf{u}^{\mathbf{T}}\mathbf{R}\mathbf{u}+2\mathbf{u}^{\mathbf{T}}\mathbf{R}\,\mathbf{B}^{\#}(.,\boldsymbol{\upsilon}_0)\mathbf{A}(\mathbf{x}(t),\boldsymbol{\upsilon},\boldsymbol{\upsilon}_0)\right) \\ & \quad -(\overline{\mathbf{u}}^{\mathrm{T}}a^2\overline{\mathbf{u}}+2\overline{\mathbf{u}}^{\mathrm{T}}\bar{a}^{-1}b^2\mathbf{A}(\mathbf{x}(t),\boldsymbol{\upsilon},\boldsymbol{\upsilon}_0)) \\ & \quad -\overline{\mathbf{u}}^{\mathrm{T}}b^2\overline{\mathbf{u}}+2a^2\overline{\mathbf{u}}^{\mathrm{T}}\overline{\mathbf{u}}+2b^2\overline{\mathbf{u}}^{\mathrm{T}}\overline{\mathbf{u}} \end{aligned} \tag{22}$$

On the other hand, the following relations are held:

$$\begin{aligned} & -\left(\mathbf{u}^{\mathbf{T}}\mathbf{R}\mathbf{u}+2\mathbf{u}^{\mathbf{T}}\mathbf{R}\,\mathbf{B}^{\#}(.,\boldsymbol{\upsilon}_0)\big(\mathbf{A}(\mathbf{x}(t),\boldsymbol{\upsilon},\boldsymbol{\upsilon}_0)\big)\right) \\ & \leq(\mathbf{B}^{\#}(.,\boldsymbol{\upsilon}_0)\big(\mathbf{A}(\mathbf{x}(t),\boldsymbol{\upsilon},\boldsymbol{\upsilon}_0)\big)^{\mathrm{T}}\mathbf{R}\,\mathbf{B}^{\#}(.,\boldsymbol{\upsilon}_0)\mathbf{A}(\mathbf{x}(t),\boldsymbol{\upsilon},\boldsymbol{\upsilon}_0) \end{aligned} \tag{23}$$

$$\begin{aligned} & -(\overline{\mathbf{u}}^{\mathrm{T}}a^2\overline{\mathbf{u}}+2\overline{\mathbf{u}}^{\mathrm{T}}\bar{a}^{-1}a^2\mathbf{A}(\mathbf{x}(t),\boldsymbol{\upsilon},\boldsymbol{\upsilon}_0))\leq \\ & \bar{a}^{-2}a^2\mathbf{A}^{\mathrm{T}}(\mathbf{x}(t),\boldsymbol{\upsilon},\boldsymbol{\upsilon}_0)\mathbf{A}(\mathbf{x}(t),\boldsymbol{\upsilon},\boldsymbol{\upsilon}_0) \end{aligned} \tag{24}$$

Finally, regarding Eqs. (23)-(24) and choosing the uncertainty bounds as Eqs. (9)-(10), it can be concluded that $\dot{\mathbf{V}}(\mathbf{x})<0$ where the necessary condition $c^2Q-2\left(a^2+b^2\right)\Omega^{\mathrm{T}}\Omega>0$ must be satisfied.

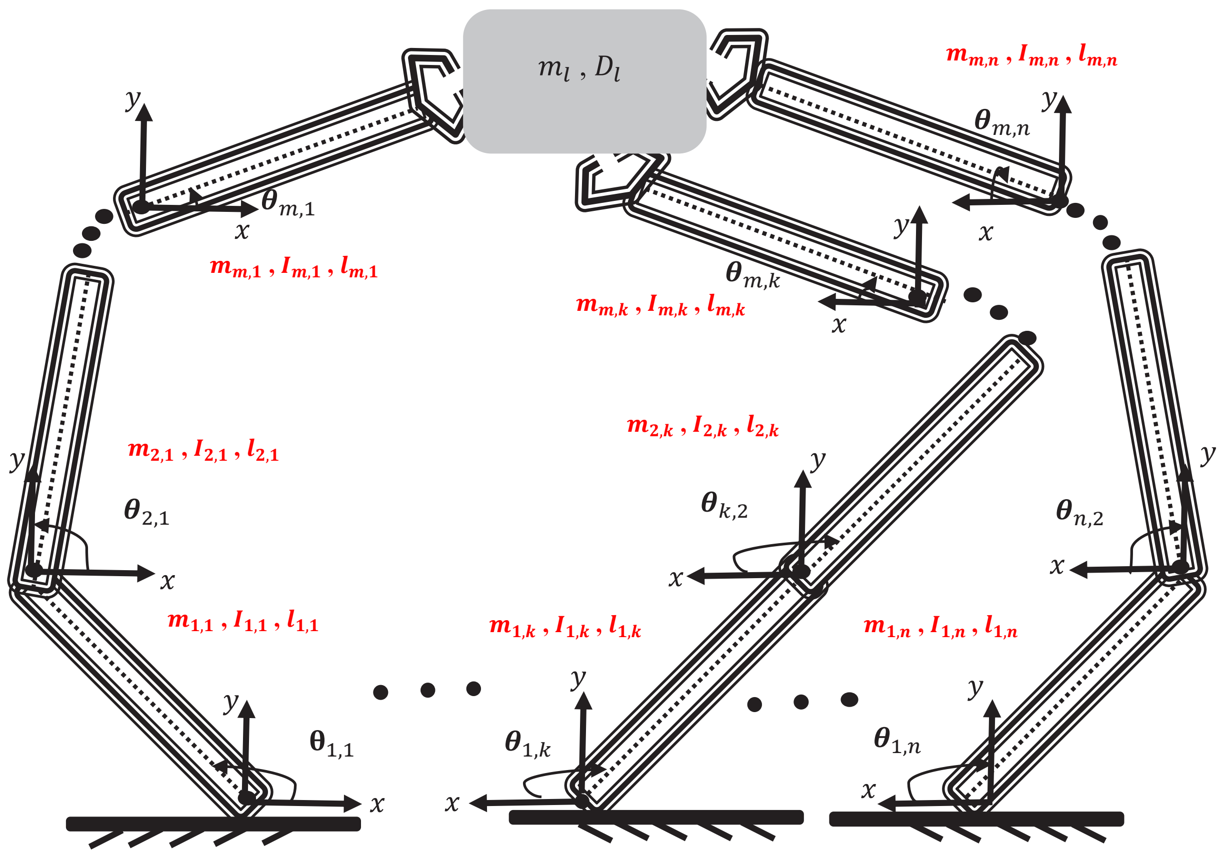

Fig. 1. Schematic view of a system of n cooperative manipulators with m link.

2- 2- Design procedure summary

We can summarize the design procedure as follows:

1- Obtain the pseudo linear formulation of the uncertain system Eq. (2)

2- Achieve the auxiliary uncertain SDC representation Eq. (3).

3- Obtain the modified cost function Eq. (6) considering upper bounds of uncertainty Eqs. (9)-(10).

4- Determine uncertainty upper bounds using the stability proof.

5- Solve the USDRE (12) to obtain optimal gain.

6- Obtain the total control input Eq. (11) and extract robust input.

7- Apply the robust input to the system with uncertainty Eq. (1).

3- Dynamics of Cooperative Manipulators

In this section, the dynamics model of cooperative manipulators shown in Fig. 1, for separate structures to be controlled and overall cooperative manipulators are presented briefly.

3- 1- Dynamics of each of cooperative manipulators

The equation of motion of the kth manipulator is as [12]:

$$\begin{aligned}&\mathbf{D}_k(\boldsymbol{\theta}_k)\ddot{\boldsymbol{\theta}}_k + \mathbf{C}_k\left(\boldsymbol{\theta}_k, \dot{\boldsymbol{\theta}}_k\right)\\&+\mathbf{G}_k(\boldsymbol{\theta}_k) + \mathbf{b}_k\left(\dot{\boldsymbol{\theta}}_k\right) = \mathbf{u}_k + \mathbf{J}_k^{\mathbf{T}}(\boldsymbol{\theta}_k)\mathbf{f}_{e,k}\end{aligned} \tag{25}$$

where $1 \le k \le n$ .The representation of each parameter is clarified as:

- $\theta_k(t) \in \mathfrak{R}^n$: vector of states
- $D_k(\theta_k) \in \mathfrak{R}^{n\times n}$: matrix of inertia
- $C_k(\theta_k, \dot{\theta}_k) \in \mathfrak{R}^n$: matrix of Coriolis and centrifugal force
- $G_k(\theta_k) \in \mathfrak{R}^n$: vector of gravity
- $b_k(\dot{\theta}_k) \in \mathfrak{R}^n$: vector of friction
- $u_k(t) \in \mathfrak{R}^n$: vector of inputs
- $J_k(\theta_k) \in \mathfrak{R}^{6\times n}$: matrix of Jacobian
- $f_{e,k} \in \mathfrak{R}^6$: vector of the external force of object to

each arm.

$J_k(\theta_k)$ and $b_k(\dot{\theta}_k)$ are defined in the appendix. Moreover, $\mathbf{f}_{e,k}$ is as [12]:

$$\mathbf{f}_{e,k}(t) = \left(\mathbf{J}_k^{\mathrm{T}}(\boldsymbol{\theta}_k)\right)^{\#} \{\mathbf{D}_k(\boldsymbol{\theta}_k)\ddot{\boldsymbol{\theta}}_k + \mathbf{C}_k(\boldsymbol{\theta}_k, \dot{\boldsymbol{\theta}}_k) + \mathbf{G}_k(\boldsymbol{\theta}_k) + \mathbf{b}_k(\dot{\boldsymbol{\theta}}_k) - \underbrace{\tilde{\mathbf{Q}}_k^{-1}\left[\left(\mathbf{J}_k^{\mathrm{T}}(\boldsymbol{\theta}_k)\right)^{\#}\right]^{\mathrm{T}} \varrho}_{\mathbf{u}_k(t)}\} \quad (26)$$

where ϱ is :

$$\varrho = \left(\sum_{k=1}^{m} \left(\mathbf{J}_k^{\mathrm{T}}(\boldsymbol{\theta}_k)\right)^{\#} \tilde{\mathbf{Q}}_k^{-1}\left[\left(\mathbf{J}_k^{\mathrm{T}}(\boldsymbol{\theta}_k)\right)^{\#}\right]^{\mathrm{T}}\right)^{-1} \times [\{\sum_{k=1}^{m} \left(\mathbf{J}_k^{\mathrm{T}}(\boldsymbol{\theta}_k)\right)^{\#} [\mathbf{D}_k(\boldsymbol{\theta}_k)\ddot{\boldsymbol{\theta}}_k + \mathbf{C}_k(\boldsymbol{\theta}_k, \dot{\boldsymbol{\theta}}_k) + \mathbf{G}_k(\boldsymbol{\theta}_k) + \mathbf{b}_k(\dot{\boldsymbol{\theta}}_k)]\} - \mathbf{f}_e(t)] \quad (27)$$

in which $\mathbf{f}_e(t)$ is obtained using [34]:

$$\begin{bmatrix} m_l \mathbf{I}_{3\times3} & \vdots & \mathbf{0}_{3\times3} \\ \cdots & \cdots & \cdots \\ \mathbf{0}_{3\times3} & \vdots & \mathbf{D}_{l3\times3} \end{bmatrix} \begin{bmatrix} \ddot{\mathbf{a}}_l(t) \\ \cdots \\ \dot{\omega}_l(t) \end{bmatrix} + \begin{bmatrix} m_l \mathbf{G} \\ \cdots \\ \omega_l(t)(\mathbf{D}_l \omega_l(t)) \end{bmatrix} = -\mathbf{f}_e(t) \quad (28)$$

where $\mathbf{I}_{3\times3}$ is the identical matrix of 3×3, $\mathbf{D}_{l3\times3}$ is the inertia matrix of the load, m_l is the mass of the load, $\mathbf{a}_l(t)$ represents acceleration vector in reference coordinates, $\omega_l(t)$ denotes angular velocity and $\dot{\omega}_l(t)$ is the vector of angular acceleration. The three rows on top of Eq. (3-133) denote Newton's second law and the next three rows present Euler's rotation equations generated from the derivation of angular momentum with respect to time $\mathbf{H}_e(t) = \mathbf{D}_l \omega_l(t)$. The gravity vector is shown by $\mathbf{G}$ where $\mathbf{G} = [0, 0, g_0]^T$ expresses that there is gravity acceleration in Z_e direction. External force $\mathbf{f}_e(t) \in \mathcal{R}_{6\times1}$ caused by the load must be divided between manipulators $\mathbf{f}_e(t) = \sum_{k=1}^{m} f_{e,k}(t)$ to assign $\mathbf{f}_{e,k}(t)$ to each arm.

3- 2- Dynamics of overall system of cooperative manipulators

The equation of motion of overall manipulators is as [12]:

$$\mathbf{D}(\boldsymbol{\theta})\ddot{\boldsymbol{\theta}} + \mathbf{C}(\boldsymbol{\theta}, \dot{\boldsymbol{\theta}}) + \mathbf{G}(\boldsymbol{\theta}) + \mathbf{b}(\dot{\boldsymbol{\theta}}) = \mathbf{u} + \mathbf{J}_k^{\mathrm{T}}(\boldsymbol{\theta})\tilde{\mathbf{f}} \quad (29)$$

where the state vector $\theta = [\theta_1(t), \ldots, \theta_m(t)]$, control input $\mathbf{u} = [\mathrm{u}_1(t), \ldots, \mathrm{u}_m(t)]$, $\tilde{\mathbf{f}}(t) = [\tilde{\mathrm{f}}_1, \ldots, \tilde{\mathrm{f}}_m]$, and $D(\theta)$, $C(\theta, \dot{\theta})$, $G(\theta)$, $b(\dot{\theta})$ and $J(\theta)$ are as:

$$\mathbf{D}(\boldsymbol{\theta}) = \begin{bmatrix} \mathbf{D}_1(\boldsymbol{\theta}_1) & \mathbf{0} & \cdots & \mathbf{0} \\ \mathbf{0} & & \ddots & \vdots \\ \vdots & & & \mathbf{0} \\ \mathbf{0} & \cdots & \mathbf{0} & \mathbf{D}_m(\boldsymbol{\theta}_m) \end{bmatrix}_{mn\times mn}$$

$$\mathbf{C}(\boldsymbol{\theta}, \dot{\boldsymbol{\theta}}) = \begin{bmatrix} \mathbf{C}_1(\boldsymbol{\theta}_1, \dot{\boldsymbol{\theta}}_1) \\ \vdots \\ \mathbf{C}_m(\boldsymbol{\theta}_m, \dot{\boldsymbol{\theta}}_m) \end{bmatrix}_{mn\times1},$$

$$\mathbf{G}(\boldsymbol{\theta}) = \begin{bmatrix} \mathbf{G}_1(\boldsymbol{\theta}_1) \\ \vdots \\ \mathbf{G}_m(\boldsymbol{\theta}_m) \end{bmatrix}_{mn\times1}$$

$$\mathbf{b}(\dot{\boldsymbol{\theta}}) = \begin{bmatrix} \mathbf{b}_1(\dot{\boldsymbol{\theta}}_1) \\ \vdots \\ \mathbf{b}_m(\dot{\boldsymbol{\theta}}_m) \end{bmatrix}_{mn\times1}$$

$$\mathbf{J}(\boldsymbol{\theta}) = \begin{bmatrix} \mathbf{J}_1(\boldsymbol{\theta}_1) & \mathbf{0} & \cdots & \mathbf{0} \\ \mathbf{0} & & \ddots & \vdots \\ \vdots & & & \mathbf{0} \\ \mathbf{0} & \cdots & \mathbf{0} & \mathbf{J}_m(\boldsymbol{\theta}_m) \end{bmatrix}_{6m\times mn}$$

and the state space form has been presented in [34].

4- Robust SDRE-based Control of Cooperative Manipulators

In this section, the proposed robust SDRE-based scheme is designed by two policies: independent control of each arm and simultaneous control of the overall system.

4- 1- Robust SDRE-based control of each of the cooperative manipulators

Considering uncertainty in SDC representation of [12] and Eq. (4) to obtain $\tilde{\mathbf{B}}_{2mn\times3mn}(x(t), \Xi_0)$, the USDC form for independent robust control of cooperative arms holding a load is obtained as:

$$\mathbf{A}_{k\,2n\times2n}(\mathbf{x}(t), \boldsymbol{\upsilon}_0) = \begin{bmatrix} \mathbf{0}_{n\times n} & \vdots & \mathbf{I}_{n\times n} \\ \cdots & \cdots & \cdots \\ \mathbf{0}_{n\times n} & \vdots & -\mathbf{D}_k^{-1}(\mathbf{x}(t), \boldsymbol{\upsilon}_0)\begin{bmatrix} \tilde{\mathbf{C}}_k(\mathbf{x}(t), \boldsymbol{\upsilon}_0) + \\ \mathrm{diag}(b_{k,1}^{v}, \ldots, b_{k,n}^{v}) \end{bmatrix} \end{bmatrix} \quad (30)$$

$$\widetilde{\mathbf{B}}_{k\,2mn\times 3mn}(\mathbf{x}(t),\boldsymbol{\upsilon}_0) = \left[\begin{matrix}\mathbf{0}_{mn\times mn}\\ \mathbf{D}_k^{-1}(\mathbf{x}(t),\boldsymbol{\upsilon}_0)\end{matrix} \;\vdots\; \left(\mathbf{I}_{2mn\times 2mn} - \begin{bmatrix}\mathbf{0}_{mn\times mn}\\ \mathbf{D}_k^{-1}(\mathbf{x}(t),\boldsymbol{\upsilon}_0)\end{bmatrix}\begin{bmatrix}\mathbf{0}_{mn\times mn}\\ \mathbf{D}_k^{-1}(\mathbf{x}(t),\boldsymbol{\upsilon}_0)\end{bmatrix}^{\#}\right)\right] \quad (31)$$

After determining USDC matrices, the next step is to solve the USDRE in Eq. (12), to obtain the gain. Then, by using Eq. (11), the augmented control is obtained. The terms could not be structured as the USDC form will be added to the control input. Finally, robust input is separated and applied to the system.

It is worth to note that since some terms in the dynamic equation of cooperative manipulators could not be extracted as USDC representation, by mimicking [12] they are added to the total control input $\mathbf{u}_{total}(t)$ as an additional term $\mathbf{u}_{k,add}(t)$ in Eq. (32).

$$\mathbf{u}_{k,add}(t) = \mathbf{G}_k(\boldsymbol{\theta}) + \mathbf{b}_k(\dot{\boldsymbol{\theta}}) - \mathbf{J}_k^{\mathrm{T}}(\boldsymbol{\theta})\tilde{\mathbf{f}}_k \quad (32)$$

Hence, for each left arm or right arm of the cooperative system, we have:

$$\mathbf{U}_k = \mathbf{u}_{total}(t) + \mathbf{u}_{k,add}(t) \quad (33)$$

Then, considering $\mathbf{U}_k = \begin{bmatrix}\mathbf{u}_k\\ \bar{\boldsymbol{u}}_k\end{bmatrix}$, $\mathbf{u}_k$ can be separated using a separation matrix [16]. In this paper $k = 1, 2$.

$k = 1$ denotes for the first or left arm and $k = 2$ denotes for the second or right arm. A similar formulation can be presented for the overall cooperative system.

An illustrative flowchart of the design process is presented in Fig. 2.

4- 2- Robust SDRE-based control of the overall system of cooperative manipulators

Considering uncertainty in SDC representation of [12] and Eq. (4) to obtain $\widetilde{B}_{2mn\times 3mn}(x(t),\Xi_0)$ the USDC form for simultaneous robust SDRE-based control of cooperative arms holding an object is achieved as:

$$\mathbf{A}_{2mn\times 2mn}(\mathbf{x}(t),\boldsymbol{\upsilon}_0) = \begin{bmatrix}\mathbf{0}_{mn\times mn} & \vdots & \mathbf{I}_{mn\times mn}\\ \cdots & \cdots & \cdots\\ \mathbf{0}_{mn\times mn} & \vdots & \mathrm{diag}\left\{\begin{matrix}-\mathbf{D}_1^{-1}(\mathbf{x}(t),\boldsymbol{\upsilon}_0)\begin{bmatrix}\tilde{\mathbf{C}}_1(\mathbf{x}(t),\boldsymbol{\upsilon}_0) +\\ \mathrm{diag}(b_{k,1}^{v},\dots,b_{k,n}^{v})\end{bmatrix},\dots,\\ -\mathbf{D}_m^{-1}(\mathbf{x}(t),\boldsymbol{\upsilon}_0)\begin{bmatrix}\tilde{\mathbf{C}}_m(\mathbf{x}(t),\boldsymbol{\upsilon}_0)\\ +\mathrm{diag}(b_{k,1}^{v},\dots,b_{k,n}^{v})\end{bmatrix}\end{matrix}\right\}\end{bmatrix} \quad (34)$$

$$\widetilde{\mathbf{B}}_{2mn\times 3mn}(\mathbf{x}(t),\Xi_0) = \left[\begin{matrix}\mathbf{0}_{mn\times mn}\\ \mathbf{D}^{-1}(\mathbf{x}(t),\boldsymbol{\upsilon}_0)\end{matrix} \;\vdots\; \left(\mathbf{I}_{2mn\times 2mn} - \begin{bmatrix}\mathbf{0}_{mn\times mn}\\ \mathbf{D}^{-1}(\mathbf{x}(t),\boldsymbol{\upsilon}_0)\end{bmatrix}\begin{bmatrix}\mathbf{0}_{mn\times mn}\\ \mathbf{D}^{-1}(\mathbf{x}(t),\boldsymbol{\upsilon}_0)\end{bmatrix}^{\#}\right)\right] \quad (35)$$

where $D(x(t),\upsilon_0) = \mathrm{diag}\{D_1(x(t),\upsilon_0),\dots,D_m(x(t),\upsilon_0)\}$. The next stages of the procedure of achieving control input are the same as the previous subsection.

5- Simulation Results

In order to verify the satisfactory performance of the robust SDRE-based control to cooperative manipulators, multiple arms in cooperation carrying a load are considered. Each arm has three DoF. The state space and specifications of the system are as given in [12]. The randomly found value of parametric uncertainty is $\chi = diag(rand(6,1))\chi_0$ in which $\chi_0 = [0.3, 0.1, 0.05, 0.5, 0.3, 0.2]$ is the upper bound for the parametric uncertainty of each arm. The first three elements of χ_0 represents uncertainty in links' length and the second three elements are uncertainty in links' mass which yields nominal SDC. $rand(6,1)$ provides a random vector with six elements which are between $[0,1]$ [35].

The design parameters and subsidiary weighting matrices for both following cases are as: $a = 15$;$b = 30$;$c = 5$;$\bar{a} = 0.5$ $\mathbf{Q}_l = 5\times 10^4[\mathbf{I}_{3\times 3} \;\vdots\; 0_{3\times 3}]$;$\mathbf{R}_l = 10^{-4}\mathrm{diag}\{0.1 \quad 0.1 \quad 1\}$; $\mathbf{Q}_r = 5\times 10^7[\mathbf{I}_{3\times 3} \;\vdots\; 0_{3\times 3}]$;$\mathbf{R}_r = 0.01\mathrm{diag}\{0.1 \quad 0.1 \quad 0.1\}$

In subsequent presented cases, we want to illustrate that different USDC formulations for separated manipulators carrying a mass and cooperative ones holding an object, result in the same outputs. However, cooperation is superior in terms of less error and control effort with the same payload. This implies that cooperation increases the DLCC. Then the proposed robust optimal scheme is compared with SDRE-based SMC to show the superiority of the proposed controller.

5- 1- Case1:

In this case, two separated arms holding an object tracking a linear path are considered. The weight of the mass for the left arm is 3.1Kg and for the right arm is 2.2 Kg. Hence, the total weight of the mass is 5.3 Kg. Load distribution between the left and right arms can be accomplished using the optimal load distribution given in [12]. However, in this paper, load distribution is accomplished by trial and error. The position and velocity of the left arm and right arm are plotted in Figs (3a) - (3d). The control inputs are depicted in Figs (3e) - (3j). Furthermore, the tracked linear path, error of end-effectors, and the norm of control inputs are illustrated in Figs. (3k), (3l) and (3m), respectively.

In order to obtain tracking error, consider a trajectory path as a line defined as [12]:

$$\begin{cases}\mathbf{X}_{des}(t) = 0\\ \mathbf{Y}_{des}(t) = 6.625t^4 - 12.125t^3 + 6.25t^2\end{cases} \quad (36)$$

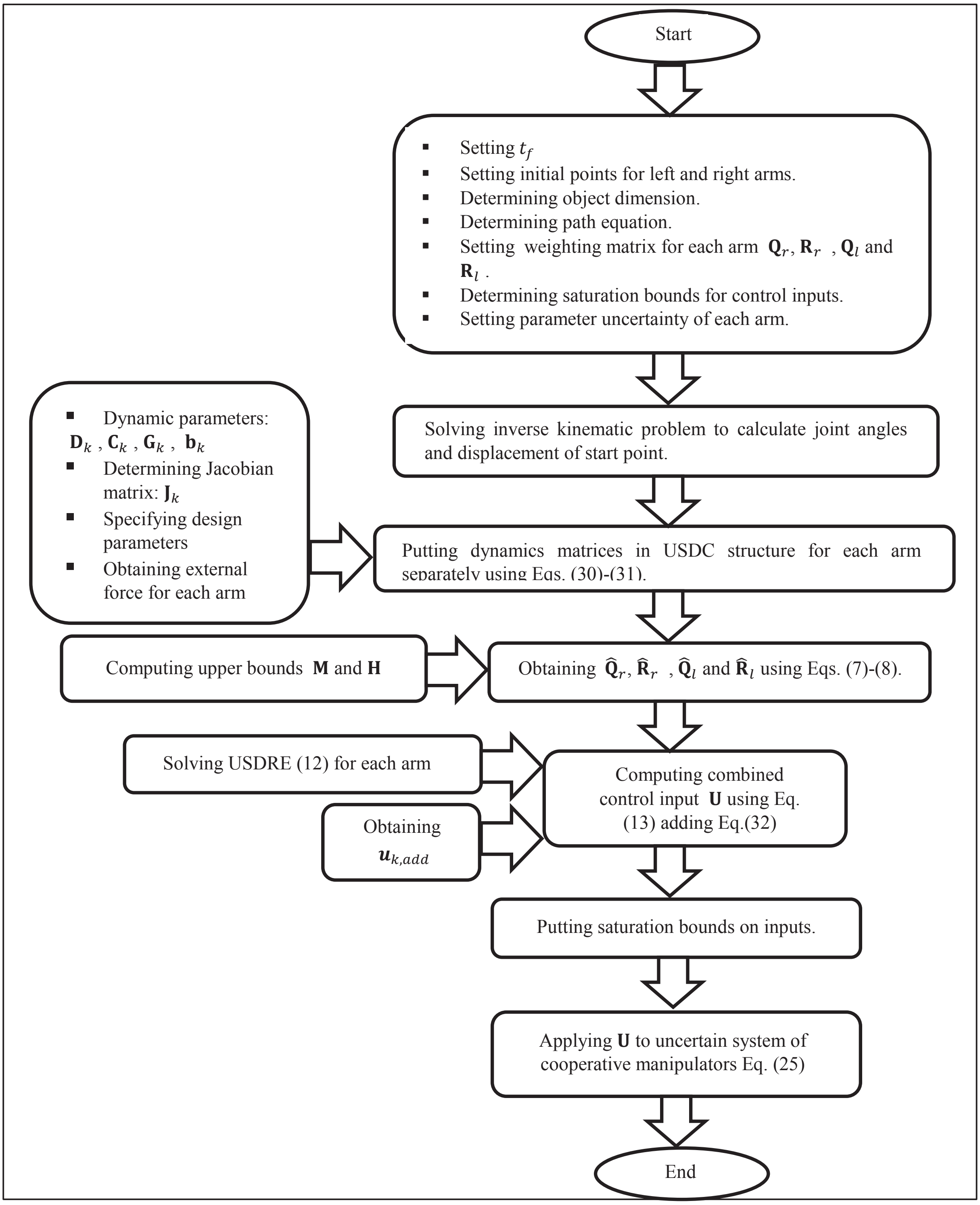

Fig. 2. Flowchart of robust SDRE-based control of cooperative manipulators holding an object

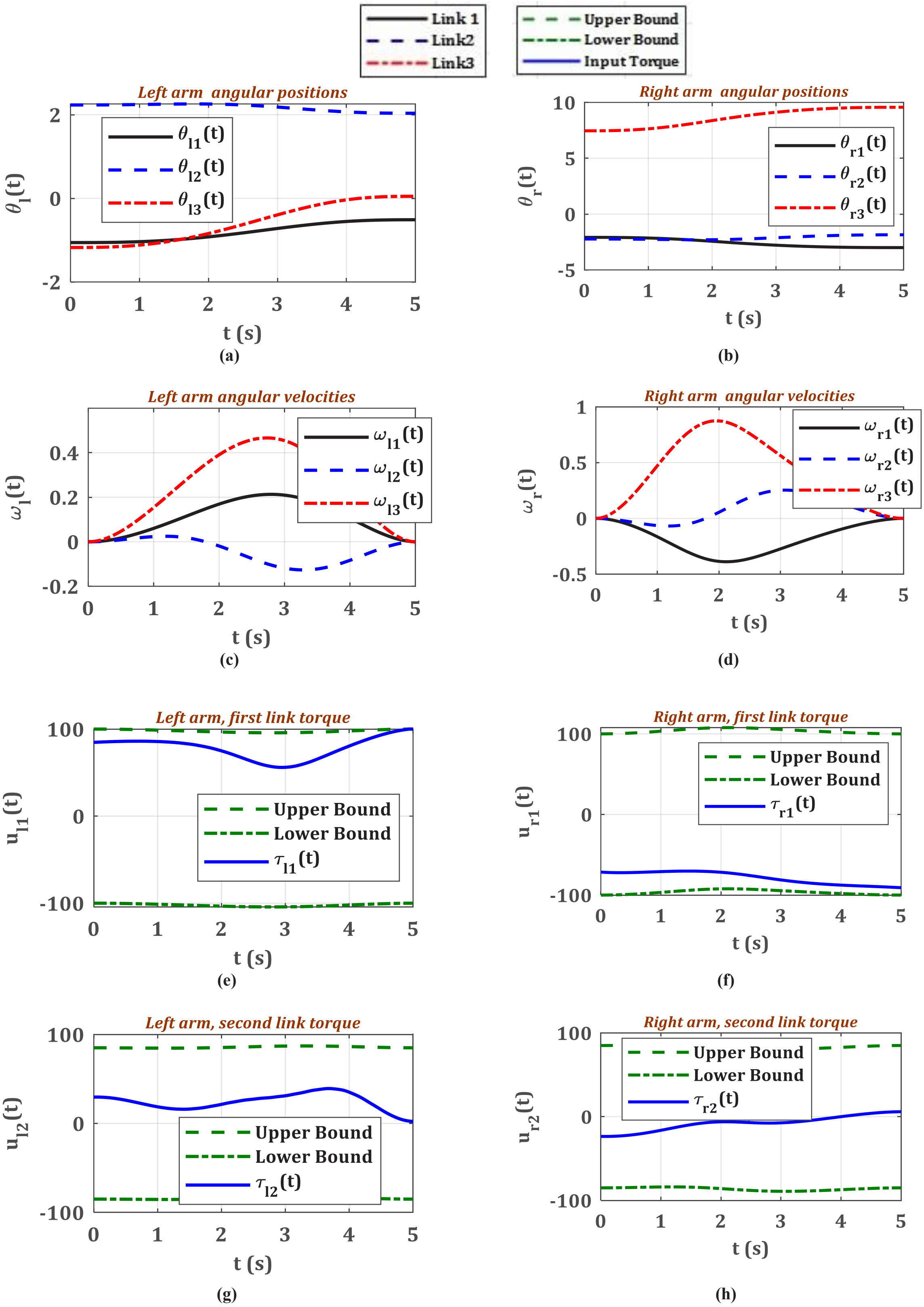

Fig. 3. Robust SDRE-based controller performance for separated multiple arms in cooperation (Continued)

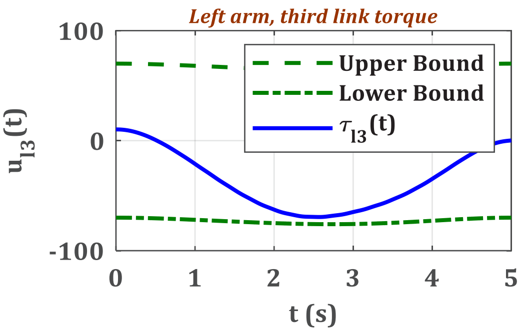

(i)

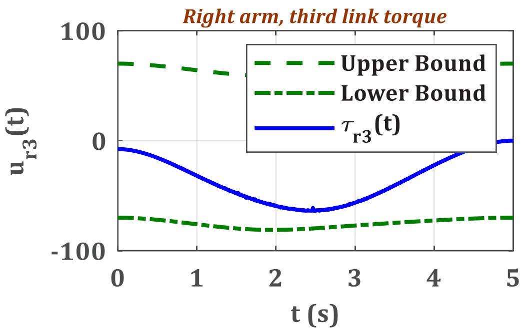

(j)

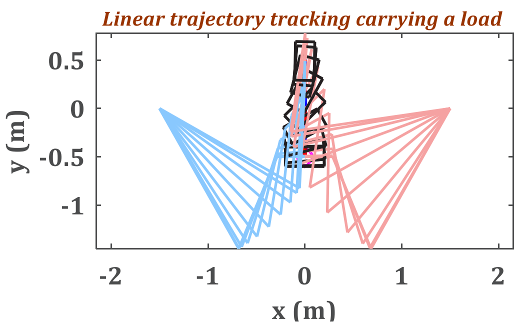

(k)

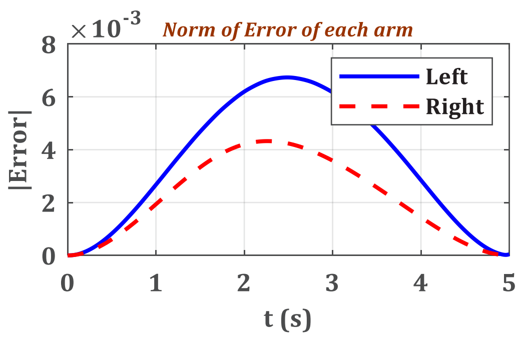

(l)

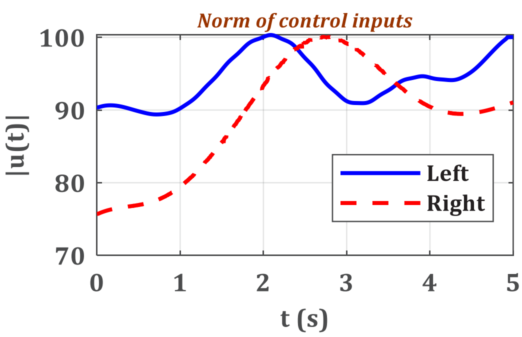

(m)

Fig. 3. Robust SDRE-based controller performance for separated multiple arms in cooperation

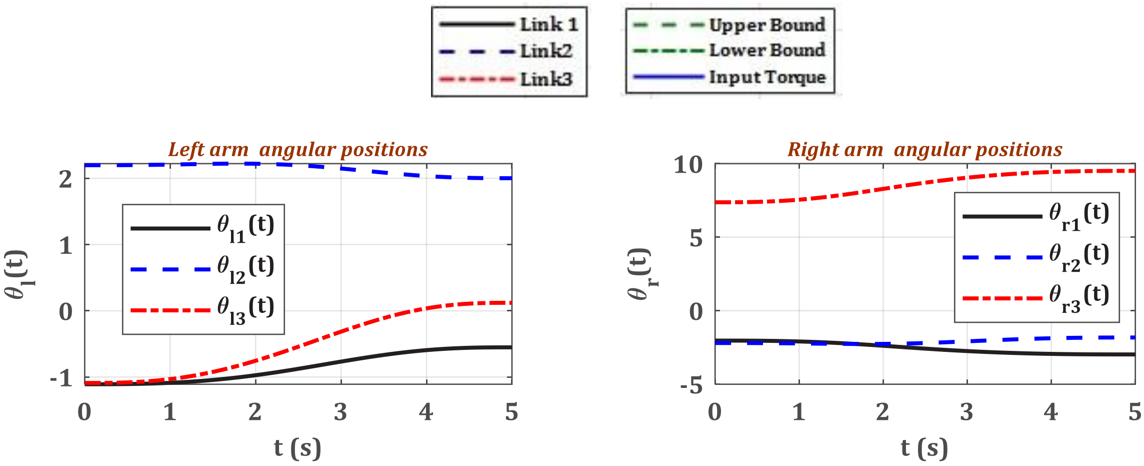

(a) (b)

Fig. 4. Robust SDRE-based controller performance for the overall system of multiple arms in cooperation (continued)

which connects the statrt point (0,-0.5)m to the end point (0,0.5)m in 5 seconds. The values for the position of the end effector in x-axis, $\mathbf{X}_e(t)$ and in y-axis, $\boldsymbol{Y}_e(t)$ are achieved using direct kinematics. The error between the end-effector of each arm and the desired linear path is obtained using:

$$Error_{left\ arm} = \sqrt{\left(\mathbf{X}_{e,l}(t) - \mathbf{X}_{des,l}(t)\right)^2 + \left(\mathbf{Y}_{e,l}(t) - \mathbf{Y}_{des,l}(t)\right)^2} \quad (37)$$

$$Error_{right\ arm} = \sqrt{\left(\mathbf{X}_{e,r}(t) - \mathbf{X}_{des,r}(t)\right)^2 + \left(\mathbf{Y}_{e,r}(t) - \mathbf{Y}_{des,r}(t)\right)^2} \quad (38)$$

The maximum value of the error norm for each arm's end-effector is gained as 67 mm for the left arm and 43 mm for the right arm. Furthermore, while the task has been completed, the control input can not be zero due to additional term $\mathbf{u}_{k,add}(t)$. Moreover, when the mass reaches the endpoint, increasing t leads to an increase in the distance between the end-effector and the final point. Hence, by increasing the distance, $\mathbf{u}(t)$ increases. However, it remains in the saturation bounds. Saturation bounds is obtained using parameters given in [12]:

$$\boldsymbol{u}_{max,m,k} = \boldsymbol{u}_{stall,m,k} - \frac{\boldsymbol{u}_{stall,m,k}}{\boldsymbol{\omega}_{nl,m,k}}\dot{\theta}_{m,k}(t), \quad m = 1,2;\ k = 1,2,3 \quad (39)$$

$$\boldsymbol{u}_{min,m,k} = -\boldsymbol{u}_{stall,m,k} - \frac{\boldsymbol{u}_{stall,m,k}}{\boldsymbol{\omega}_{nl,m,k}}\dot{\theta}_{m,k}(t), \quad m = 1,2;\ k = 1,2,3 \quad (40)$$

where $u_{stall,m,k}$ is stall torque and $\omega_{nl,m,k}$ is no load speed of the motor of kth link of mth manipulator.

5- 2- Case2:

In this case, two arms in cooperative form holding an object which is 5.3 kKg, tracking a linear path is considered. The position and velocity of the left arm and right arm are plotted in Figs (4a) - (4d). The control inputs are depicted in Figs (4e) - (4j). Furthermore, the tracked linear path, error of end-effectors, and input norm are illustrated in Figs (4k)- (4m). The difference between this case and the previous one is that in this case, the total mass (5.3 kg) is holding cooperatively and the robotic system is tracking a linear trajectory between two points. The objective is reaching the endpoint carrying

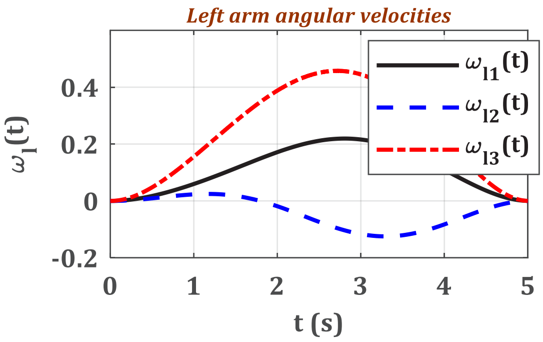

(c)

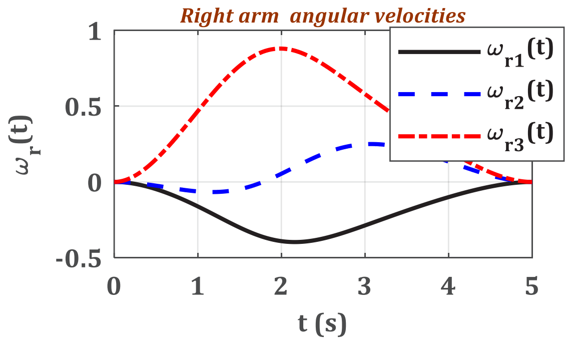

(d)

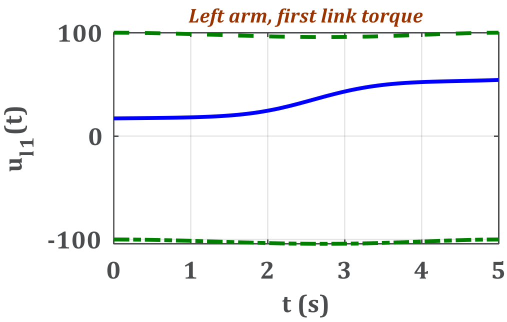

(e)

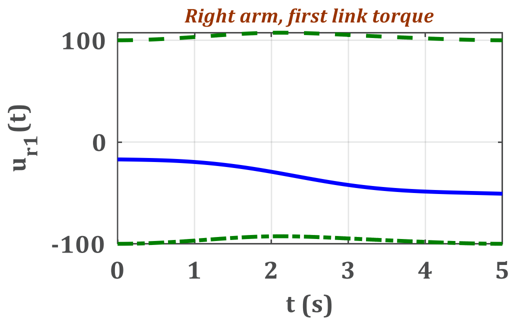

(f)

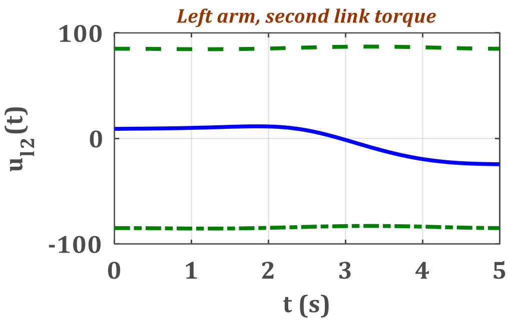

(g)

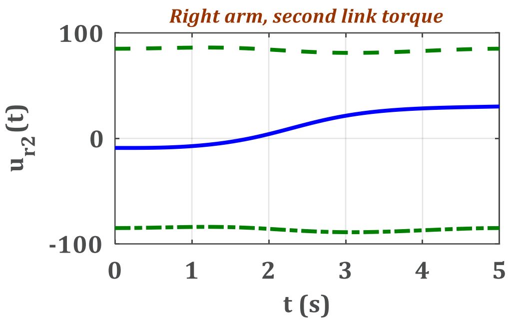

(h)

Fig. 4. Robust SDRE-based controller performance for the overall system of multiple arms in cooperation (continued)

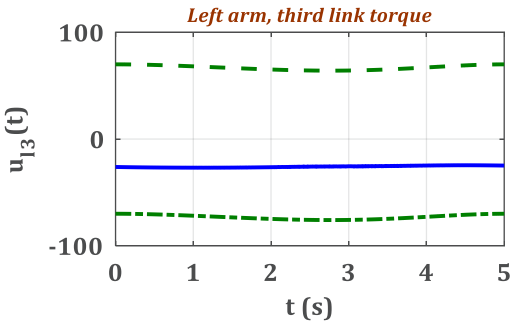

(i)

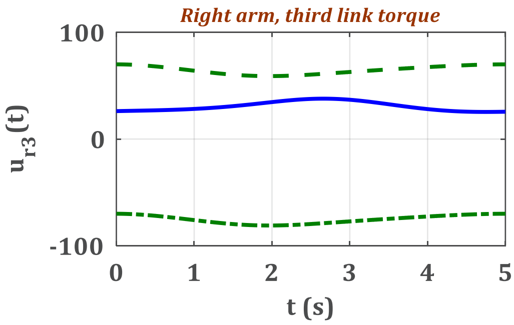

(j)

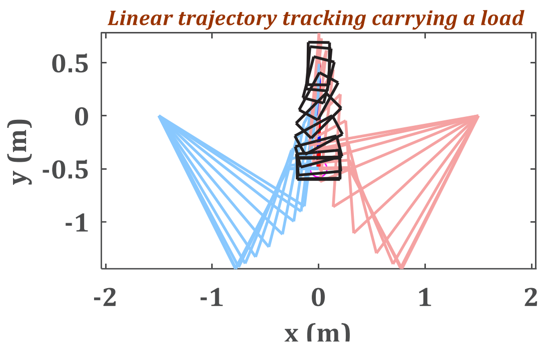

(k)

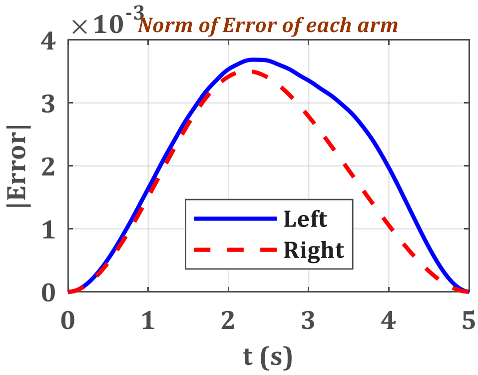

(l)

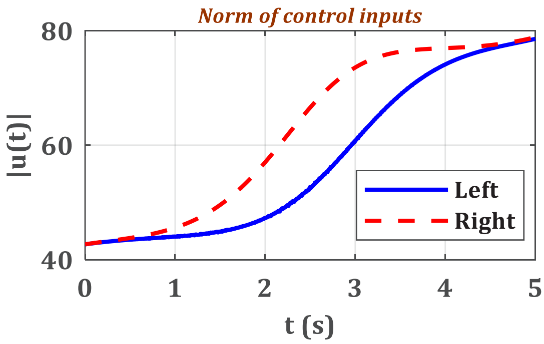

(m)

Fig. 4. Robust SDRE-based controller performance for the overall system of multiple arms in cooperation

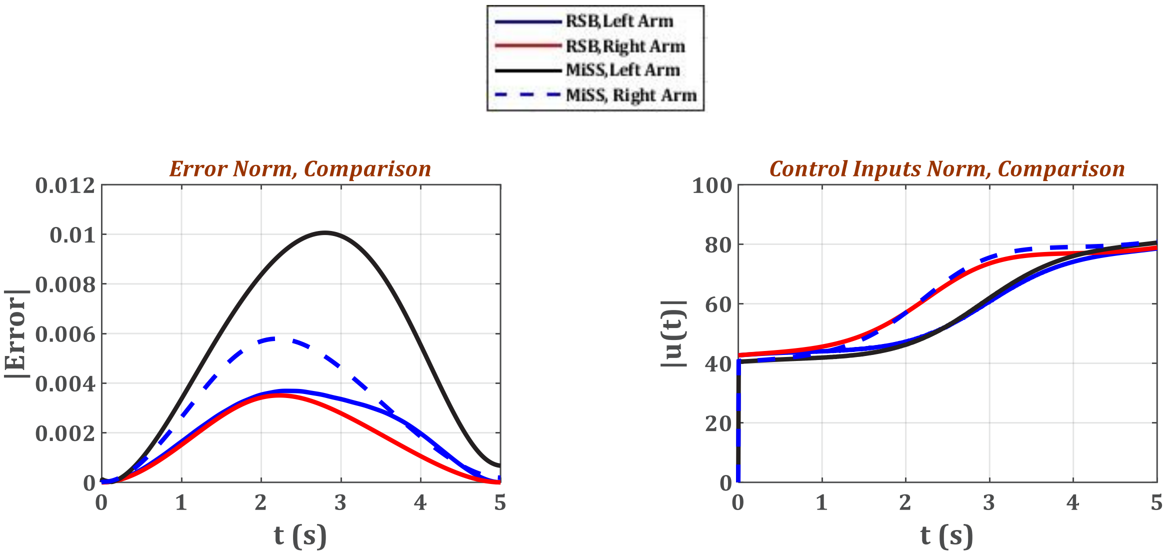

(a) (b)

Fig. 5. Comparison of the robust SDRE-based controller and MiSS performance for the overall system of multiple arms in cooperation (RSB denotes the proposed Robust SDRE-Based control)

the object. However, in the previous case, the total mass is distributed between the left and the right arm and they separately carry the load along the linear trajectory toward the final point. The angular positions illustrated in Figs. (4a) and (4b) for the end-effectors are gained using inverse kinematics for the start point and end point. Saturation bounds in Figs. (4e), (4f),(4g),(4h),(4i),(4j), for inputs are achieved utilizing Eqs. (39)- (40).

The maximum numerical values for error norm considering Eqs. (37) and (38) for each arm's end-effector is gained 37 mm for the left arm and 35 mm for the right arm. Comparing the previous case, handling a 5.3 kg mass, with cooperation leads to a decrease in error norms and control inputs of manipulators. Hence, cooperation increases DLCC.

5- 3- Discussion on Simulation Results

Regarding simulation results, the robust SDRE-based controller has a satisfactory performance in controlling such a complicated nonlinear robotic system in tracking a path holding an object. The error is negligible in both cases and control inputs are inside the saturation bounds. Moreover, comparing two cases, possessing similar total payload (5.3 Kg), the same design parameters, and subsidiary weighting matrices, cooperation enhances the performance of manipulators in terms of negligible error and smaller control efforts. This is obvious by considering numerical values presented for each case and comparing end-effectors' errors and input norms in Figs (3l) and (3m) with Figs (4l) and (4m). As a result, cooperation leads to an increase in DLCC.

Moreover, comparing the results of the proposed robust controller and Mixed SDRE-SMC [19] for the second case, the superior performance of robust SDRE-based control can be easily observed as illustrated in Fig. 5.

The numerical performance indices for each arm to compare the proposed scheme and MiSS are presented in Table 2.

6- Conclusion

In this paper, an USDRE framework was employed to cope with the difficulty introduced by robust controller design for cooperative manipulators handling an object. To design the proposed robust controller, a subsidiary sub-optimal problem with a modified performance index was solved. By separating the robust input, the robust control problem was solved with considerable facility. Simulation results on the system of multiple arms in cooperation carrying a load easily validate the efficient performance of the proposed scheme as well as the superiority of cooperation compared with a separate robust control strategy. Furthermore, the proposed scheme is superior versus MiSS as illustrated in the simulation results.

Table 2. Comparison the SDRE-based scheme and MiSS [19]

Performance Index / Controller	$max\|\|Error\|\|$ for Left arm	$max\|\|Error\|\|$ for Right arm	$max\|\|u\|\|$ for Left arm	$max\|\|u\|\|$ for Right arm
Proposed scheme	**0.0037**	**0.0035**	**78.79**	**78.77**
MiSS[19]	**0.0100**	**0.0058**	**80.91**	**80.97**

References

[1] D.E. Kirk, Optimal control theory: an introduction. New York: Dover Publications, 2004.

[2] H.N. Foghahayee, and M.B. Menhaj, “A near nonlinear optimal controller for the nonlinear inverted pendulum,” in Proc. 2016 4th Int. Conf. on Cont., Ins., and Aut. (ICCIA), pp. 273-278.

[3] M.N. Monfared, A. Fakharian, and M.B. Menhaj, “A new modified polynomial-based optimal control design approach,” Proc. of the Ins.of Mech. Eng., Part I: J. of Sys. and Contr. Eng., vol. 235, pp. 355-370, 2021.

[4] E. Al’Brekht, “ On the optimal stabilization of nonlinear systems,” J. Appl. Math. Mech., vol. 25, pp. 1254–1266, 1961.

[5] C.L Navasca, and A.J. Krener, “Solution of Hamilton Jacobi Bellman equations,” in Proc. of 2000 39th IEEE conf. on dec. and cont.l (Cat no.00CH37187), Sydney, NSW, Australia, pp.570–574.

[6] A. Fakharian, and M.T. H. Beheshti, “Solving linear and nonlinear optimal problem using modified Adomian decomposition method,” J. of Comp. and Rob., vol. 1, pp. 1 -8, 2010.

[7] M.E. Dehshalie, M.B. Menhaj, and M. Karrari, “Fault tolerant cooperative control for affine multi-agent systems: an optimal control approach,” J Franklin Inst., vol. 356, pp. 1360–1378, 2019.

[8] B. Luo, H.N. Wu, T. Huang, et al., “Reinforcement learning solution for HJB equation arising in constrained optimal control problem,” Neu. Netw., vol. 71, pp. 150–158, 2015.

[9] I. Hwang, J. Li, and D. Du, “Differential transformation and its application to nonlinear optimal control,” J. Dyn. Syst. Meas. Contr., vol. 131: 051010. 2009.

[10] T. Cimen, “State-dependent Riccati equation (SDRE) control: a survey,” IFAC P , vol. 41, pp. 3761–3775. 2008.

[11] M.H. Korayem, N.Y. Lademakhi, and S.R. Nekoo , “Application of the state-dependent Riccati equation for flexible-joint arms: Controller and estimator design,” Optimal Control Applications and Methods. vol 39, pp. 792-808, 2018.

[12] M. H. Korayem, and S. R. Nekoo, “Controller design of cooperative manipulators using state-dependent Riccati equation,” Robotica, vol. 36, pp. 484-515, 2018.

[13] N.Nasiri, and N.Y. Lademakhi, “Nonlinear combined SMC-SDRE control versus SMC and SDRE approaches for electrical flexible-joint robots based on optimal observer”, 2021 9th RSI Int. Conf. on Rob. and Mechat. (ICROM), pp. 568-573.

[14] R. Shadi, F. B. Liavoli and A. Fakharian, “Nonlinear Sub-Optimal Controller for Ebola Virus Disease: State-Dependent Riccati Equation Approach,” in Proc. 2021 7th Int. Conf. on Cont., Inst. and Aut. (ICCIA), pp. 1-6.

[15] F. Lotfi, S. Ziapour, F. Faraji, and H. D. Taghirad, “ A switched SDRE filter for state of charge estimation of lithium-ion batteries,” Int. J. Elec. Pow. Ener. Sys., vol. 117, pp.1-10, 2020.

[16] N. Nasiri, A. Fakharian, and M.B. Menhaj, “Observer-based robust control for flexible-joint robot manipulators: A state-dependent Riccati equation-based approach,” Trans. I. Meas. Contr., vol. 42, pp. 3135–3155, 2020.

[17] N. Nasiri, A. Fakharian, and M.B. Menhaj, “A novel controller for nonlinear uncertain systems using a combination of SDRE and function approximation technique: Regulation and tracking of flexible-joint manipulators,” J. Frankl. I., vol. 358, pp. 5185-5212, 2021.

[18] A. H. Korayem, S. R. Nekoo and M. H. Korayem, “Sliding mode control design based on the state-dependent Riccati equation: theoretical and experimental implementation,” Int. J. of Control., vol. 92, pp. 2136-2149, 2019.

[19] A. H. Korayem, S. R. Nekoo and M. H. Korayem, “Optimal sliding mode control design based on the state-dependent Riccati equation for cooperative manipulators to increase dynamic load carrying capacity,” Robotica, vol. 37, pp. 321-337, 2019.

[20] [20]Y.L. Kuo, “Robust chaos synchronizations using an SDRE-based sub-optimal control approach,” Nonlin.

Dyn., vol. 76, pp. 733-742, 2014.

[21] N.Nasiri, H. Sadjadian, and A.M.Shahri, "Nonlinear Stabilizing Controller for a Special Class of Single Link Flexible Joint Robots", J. of Comp. and Rob., vol 5, pp. 37-42, 2012.

[22] N.Nasiri, A. Fakharian, M.B. Menhaj, "State-Dependent Differential Riccati Equation: A novel Application to Finite-Time Robust Tracking Control of Flexible-Joint Manipulators" , Submitted to: ISA Transactions.

[23] S.R. Nekoo, "Model reference adaptive state-dependent Riccati equation control of nonlinear uncertain systems: regulation and tracking of free-floating space manipulators," Aerospace Science and Technology, vol. 84, 348-360, 2019.

[24] N. Nasiri, H. Sadjadian, and A. M. Shahri, "Voltage-based control of a flexible-joint electrically driven robot using backstepping approach," 2013 4th Annu. Int. Pow. Elec., Drive Sys. and Tech. Conf. (PEDSTC), pp 541-546.

[25] A. Izadbakhsh, and M.M. Fateh, "Robust Lyapunov-based control of flexible-joint robots using voltage control strategy," Arab. J. Sci. Eng., vol. 39, pp. 3111–3121, 2014.

[26] A. Izadbakhsh, "Robust control design for rigid-link flexible-joint electrically driven robot subjected to constraint: theory and experimental verification ," Nonlin. Dyn., vol. 85, pp. 751–765, 2016.

[27] A. Izadbakhsh, and S. Khorashadizadeh, "Robust control design for rigid-link flexible-joint electrically driven robot subjected to constraint: theory and experimental verification ," Rob. and Nonlin. Cont., vol. 30, pp. 2719–2735, 2020.

[28] M. H. Korayem, and S. R. Nekoo, "Non-linear suboptimal SDRE controller for cooperative manipulators to increase dynamic load carrying capacity," 2015 3th RSI International Conference on Robotics and Mechatronics (ICROM), pp. 19-24.

[29] J. H. Barragan, C. L. Franco, A. Y, Alanis, N. A. Daniel, and M. L. Franco, "Dual-arm cooperative manipulation based on differential evolution," Int. J. of Adv. Rob. Sys., vol. 16, 2019.

[30] A. Izadbakhsh, N. Nikdel, and A. Deylami, "Cooperative and robust object handling by manipulators based on the differential equation approximator," ISA Trans.,in press.

[31] A. Deylami, and A. Izadbakhsh, "FAT-based robust adaptive control of cooperative multiple manipulators without velocity measurement,"Robotica, pp.1-31, 2021.

[32] A. Izadbakhsh, N. Nasiri, M.B. Menhaj,"Linear/nonlinear PID control of cooperative multiple robot manipulators: A robust approach," AUT J. of Modelling and Simulation, vol. 55, pp.1-5, 2023.

[33] F. Lin, Robust control design: An optimal control approach. New Jersey: John Wiley &Sons.,2007.

[34] C. J. Li, "Coordinated motion control of multi-arm robot systems with optimal load distribution," Syst. Control Lett., vol. 15, pp. 237–245, 1990.

[35] S.R. Nekoo, A. Ollero, "A robust state-dependent Riccati equation controller with parameter uncertainty and matched disturbance," J. Franklin Ins., vol. 360, pp. 14584-14595, 2023.

[36] R.J. Schilling, " Fundamentals of robotics analysis and control", Prentice Hall, New Delhi, 2003.

Appendix A

Friction of *m*th link of *k*th arm is as given in [12], [36]:

$$b_{k,m}\left(\dot{\theta}_{k,m}(t)\right) = b_{k,m}^{v}\dot{\theta}_{k,m}(t) + sgn\left(\dot{\theta}_{k,m}(t)\right)\left[b_{k,m}^{v} + (b_{k,m}^{s} - b_{k,m}^{d})\exp(\frac{-\left|\dot{\theta}_{k,m}(t)\right|}{\varepsilon})\right] \quad (1\text{-A})$$

For $k = 1{,}2$ and $1 \leq m \leq 3$, $b_{k,m}^{v}$ is viscous friction, $b_{k,m}^{d}$ is dynamic friction, $b_{k,m}^{s}$ is static friction and ε denotes for small positive constant. Moreover, matrix of Jacobian $\mathbf{J}_k(\boldsymbol{\theta}_k)$ is as given in [12]:

$$\mathbf{J}_k(\boldsymbol{\theta}_k) = \begin{bmatrix} a1 & a2 & a3 \\ a4 & a5 & a6 \\ 0 & 0 & 0 \\ 0 & 0 & 0 \\ 0 & 0 & 0 \\ 1 & 1 & 1 \end{bmatrix} \quad (2\text{-A})$$

where:

$$a1 = -l_{k2}\sin(\theta_{k1}+\theta_{k2}) - l_{k1}\sin(\theta_{k1}) - l_{k3}\sin(\theta_{k1}+\theta_{k2}+\theta_{k3})$$

$$a2 = -l_{k2}\sin(\theta_{k1}+\theta_{k2}) - l_{k3}\sin(\theta_{k1}+\theta_{k2}+\theta_{k3})$$

$$a3 = -l_{k3}\sin(\theta_{k1}+\theta_{k2}+\theta_{k3})$$

$$a4 = l_{k2}\cos(\theta_{k1}+\theta_{k2}) + l_{k1}\cos(\theta_{k1}) + l_{k3}\cos(\theta_{k1}+\theta_{k2}+\theta_{k3})$$

$$a5 = l_{k2}\cos(\theta_{k1}+\theta_{k2}) + l_{k3}\cos(\theta_{k1}+\theta_{k2}+\theta_{k3})$$

$$a6 = l_{k3}\cos(\theta_{k1}+\theta_{k2}+\theta_{k3})$$

HOW TO CITE THIS ARTICLE
N. Nasiri, A. Fakharian, M. B. Menhaj, An SDRE- Suboptimal Framework for Robust Control of Multiple Arms Carrying a Load in Cooperation , AUT J. Model. Simul., 55(2) (2023) 299-316.

DOI: 10.22060/miscj.2024.22649.5337